

Algorithmic Obfuscation for LDPC Decoders

Jingbo Zhou and Xinmiao Zhang, *Senior Member, IEEE*

Abstract—In order to protect intellectual property against untrusted foundry, many logic-locking schemes have been developed. The main idea of logic locking is to insert a key-controlled block into a circuit to make the circuit function incorrectly without right keys. However, in the case that the algorithm implemented by the circuit is naturally fault-tolerant or self-correcting, existing logic-locking schemes do not affect the system performance much even if wrong keys are used. One example is low-density parity-check (LDPC) error-correcting decoder, which has broad applications in digital communications and storage. This paper proposes two algorithmic-level obfuscation methods for LDPC decoders. By modifying the decoding process and locking the stopping criterion, our new designs substantially degrade the decoder throughput and/or error-correcting performance when the wrong key is used. Besides, our designs are also resistant to the SAT, AppSAT and removal attacks. For an example LDPC decoder, our proposed methods reduce the throughput to less than 1/3 and/or increase the decoder error rate by at least two orders of magnitude with only 0.33% area overhead.

Index Terms—Fault tolerant, Hardware security, Logic locking, LDPC decoder, Stopping criterion

I. INTRODUCTION

LOGIC locking [1] can help to protect intellectual property of a circuit by inserting a key-controlled block. The circuit does not function correctly without a right key. The satisfiability (SAT) attack [2] is the most powerful attack that can decrypt many logic-locking schemes [1], [3]–[6]. Its main idea is to apply Boolean SAT solvers to solve and update the conjunctive normal form (CNF) formula of target obfuscated circuit iteratively to get distinguishing input patterns (DIPs). The DIP found in each iteration is utilized to query a functioning chip to get the corresponding correct output. Then the keys that make the circuit output different from the correct output are excluded. After all the wrong keys are excluded, the attacker can get the right keys.

The Anti-SAT [7] and SARlock [8] schemes make the number of iterations needed by the SAT attack exponential. However, both of them are composed of large AND/NAND trees, which make them subject to the approximate (App-) SAT attack [9]. In addition, the large AND/NAND trees can be identified and replaced by removal attacks [10]. By increasing the corruptibility of all wrong keys, the Diversified Tree Logic (DTL) design [9] achieves better resistance to the AppSAT attack at the cost of degraded resiliency to the SAT attack. Different from the Anti-SAT [7] and SARlock [8] that require no overlap among the sets of wrong keys excluded by different DIPs, the Generalized (G-) Anti-SAT design [11] allows overlap among the sets. It can be built by using a large number of possible functions instead of AND/NAND trees. As

The authors are with The Ohio State University, Columbus, OH 43210, USA. Emails: {zhou.2955, zhang.8952}@osu.edu.

a result, the G-Anti-SAT design is more resilient to removal attacks. Besides, it achieves better resistance to the AppSAT attack without sacrificing the resistance to the SAT attack. The recently proposed Cascade (CAS)-Lock scheme [12] is a special case of the G-Anti-SAT design.

The strip functionality logic locking (SFLL) [13] scheme corrupts the original circuit and adds a logic-locking block to correct the corrupted original circuit when right keys are applied. Different from the other logic-locking schemes, the circuit does not function correctly if the key-controlled block is removed and its output is replaced by a constant signal. Hence, the SFLL can more effectively resist removal attacks. However, the functional analysis on logic locking (FALL) [14] method can successfully attack the SFLL by analyzing its functional and structural properties.

In systems that are fault-tolerating or self-correcting, errors happened on the signals may not affect the overall output or may get corrected by later computations. Examples are low-density parity-check (LDPC) codes [15], machine learning, and approximate computing. For the circuits implementing these algorithms, even if a logic-locking scheme is used and a signal is flipped when wrong keys are applied, the overall performance may not be affected much. To substantially degrade the performance when the key is incorrect, the obfuscation scheme needs to be designed using the properties of the algorithm. Algorithmic logic locking has been developed [16] for circuits implementing fault-tolerating machine learning algorithms by utilizing the statistics of the inputs. In this paper, for the first time, algorithmic approaches are investigated to obfuscate self-correcting decoders of LDPC codes, which are the most extensively-used error-correcting codes in digital communication and storage systems. Given the probability information from the communication or storage channel, LDPC decoder iteratively updates probability messages according to the parity check matrix that defines the code. At the end of each iteration, the decoder checks if a codeword is found to decide whether to stop. Even if message bits get flipped, later decoding iterations may not be affected at all or a few more iterations are needed to correct them.

This paper proposes two algorithmic-level obfuscation methods for LDPC decoders. Both of them replace the original stop condition checking part with a key controlled logic-locking block. The first one makes the decoding process run until the last iteration in most cases, when the wrong key is used. Accordingly the decoder throughput is reduced substantially. At the cost of larger overhead, the second scheme is designed so that most of the wrong keys have high corruptibility. As a result, it leads to substantial degradation on not only the throughput but also the error-correcting performance when the key is incorrect. Additionally, low-overhead modifications on the LDPC decoding algorithm are developed in this paper to

change the correct decoding stop condition so that the correct key can not be guessed. The proposed schemes effectively resist the SAT and AppSAT attacks. Even if a key is returned by the attacks, it makes the throughput substantially lower and is not usable. Our design is also resistant to removal attacks. Even if the logic-locking block is identified from the netlist, the attacker is not able to replace it to make the decoder function correctly since the correct stop condition has been modified and is unknown to the attacker. For an example (1270, 635) LDPC decoder, our proposed methods reduce the throughput to less than 1/3 and/or increase the decoder error rate by at least two orders of magnitude at practical channel conditions. The first and second proposed designs only increase the area requirement by 0.09% and 0.33%, respectively, without any penalty on the achievable clock frequency.

This paper is organized as follows. Section II briefly introduces major attacks, existing logic-locking schemes, and LDPC codes. Section III proposes two algorithmic obfuscation methods for LDPC decoders. The security and complexity overhead analyses of the proposed schemes are presented in Section IV. Conclusions follow in Section V.

II. BACKGROUNDS

This section introduces basic knowledge on logic locking, various attacks, and LDPC codes.

A. SAT and AppSAT attacks

The SAT attack model assumes that the attacker has access to: 1) the locked netlist of the chip; 2) an activated chip with the correct key input. The netlist of the locked circuit can be represented by $Y = f_e(X, K)$, where X , K and Y are the primary input, key input, and primary output vector, respectively. Its CNF formula is represented by $C_e(X, K, Y)$. Denote the function of the activated chip by $Y = f_o(X)$. The SAT attack finds the correct keys by excluding all wrong keys that make the output different from the original output by utilizing DIPs. Initially, the CNF formula is

$$F_0 := C_e(X, K_1, Y_1) \wedge C_e(X, K_2, Y_2) \wedge (Y_1 \neq Y_2) \quad (1)$$

The SAT solver is applied on this formula to solve for X that leads to different output Y_1 and Y_2 under different keys K_1 and K_2 . This X is referred to as a DIP and is denoted by X_1^d . Then the correct output is derived by querying the activated circuit as $Y_1^d = f_o(X_1^d)$. After that, new constraints are added to (1), and the initial CNF formula is updated to $F_1 = F_0 \wedge C_e(X, K_1, Y_1^d) \wedge C_e(X, K_2, Y_2^d)$. Then, the updated CNF formula is solved for another DIP X_2^d , which is used to query the activated circuit and update the CNF formula again. This process is repeated iteratively. In the i -th iteration, the CNF formula is $F_i = F_0 \wedge \bigwedge_{j=1}^i (C_e(X, K_1, Y_j^d) \wedge C_e(X, K_2, Y_j^d))$. If F_i is satisfiable, then not all wrong keys have been excluded from the key space. When the CNF formula is no longer satisfiable, say after λ iterations, the algorithm stops. At this

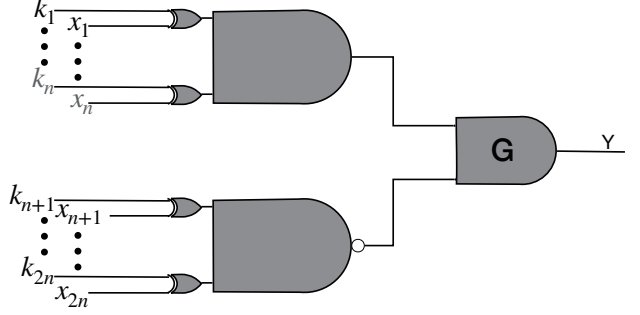


Fig. 1. Anti-SAT logic-locking block

time, the correct keys can be derived by solving the following CNF formula.

$$F := \bigwedge_{j=1}^{\lambda} (C_e(X, K_1, Y_j^d) \wedge C_e(X, K_2, Y_j^d))$$

The AppSAT attack [9] is a technique developed based on the SAT attack. In this attack, after every certain number of iterations, random input patterns are utilized to query the activated chip and get the portion of the input patterns generating the wrong output. The constraints from these queries are also added to the CNF formula each time. If the portion falls below a threshold for a number of rounds, the AppSAT algorithm terminates and returns a key from the remaining keys as the approximate key. Define the corruptibility of a wrong key as the number of input patterns that make the output different from the original output when the wrong key is applied. The wrong keys with higher corruptibility are more likely to be excluded by the AppSAT attack.

B. SAT-resistant logic-locking schemes

The Anti-SAT block proposed in [7] is composed of two AND/NAND trees sharing the same n -bit input X as shown in Fig. 1. Any $[k_1, k_2, \dots, k_n] = [k_{n+1}, k_{n+2}, \dots, k_{2n}]$ are correct keys, and '0' is the correct output. The number of iterations needed by the SAT attack is $\lambda = 2^n$. However, the corruptibility of each wrong key is only one. Using a random key will only lead to the wrong output for one input pattern.

The constraint to resist the SAT attack in the Anti-SAT scheme is very strict. The set of wrong keys excluded by each input pattern does not have overlap. The G-Anti-SAT scheme [11] generalized the SAT-resistance constraint. The wrong key sets are allowed to have overlap and each input pattern must exclude at least one unique wrong key. These generalizations enable a large number of various functions instead of AND and NAND trees to be utilized to implement the blocks and still guarantee that the number of iterations needed by the SAT attack is $\lambda = 2^n$. The overlaps among the wrong key sets also allow a large portion of the wrong keys to have high corruptibility. As a result, the chance that the AppSAT attack returns a low-corruptibility wrong key is reduced.

The DTL design [9] replaces some AND gates in AND/NAND tree shown in Fig. 1 by OR or XOR gates to increase the corruptibility of all wrong keys. Although this

means better resistance to the AppSAT attack, the number of iterations needed by the SAT attack in the DTL design is compromised and is reduced by a factor of the corruptibility value.

C. Removal attacks

Different from the SAT and AppSAT attacks, removal attacks try to locate the logic-locking block and nullify its effect. The removal attack in [10] utilizes signal probability skews (SPSs). The SPS of a signal x is defined as $s_x = \Pr[x = 1] - 0.5$. For a large AND/NAND tree, the absolute difference between the SPSs (ADS) of the two inputs of the last gate is close to one. On the other hand, the ADS values of the other gates in a normal circuit are much lower. Hence, the last gate of the Anti-SAT block in Fig. 1 can be identified by sorting the ADS values and its output can be replaced by ‘0’ to make the locked circuit function correctly.

The G-Anti-SAT design can replace the AND/NAND functions in Fig. 1 with a variety of functions and the last gate can not be easily identified by sorting the ADS values. However, AND/NAND gates with a large number of inputs are still needed to make each wrong key set have a unique wrong key. They have the largest absolute SPS values and can be found by the gate removal attack in [17]. Even though these AND/NAND gates are not the last gate of the lock-locking block, removing them makes the G-Anti-SAT more vulnerable to the SAT attack.

The SFLL is proposed in [13] to resist removal attacks. It first corrupts a signal in the circuit to make the overall output wrong under selected input patterns. Then, a key-controlled logic-locking block is added to correct that signal when right keys are applied. Even though the key-controlled block can be identified and removed, the original signal has been corrupted and hence the circuit still cannot function correctly under those selected input patterns. Nevertheless, the circuit is corrupted using a Hamming distance checker in the SFLL. By utilizing the properties of this function, the FALL attack [14] can recover the right key used in the SFLL.

D. LDPC decoder

LDPC codes are linear block error-correcting codes, which can be specified by the parity check matrix H . An (n, s) code encodes s -bit messages to n -bit codewords. A vector $c = [c_0, c_1, \dots, c_{n-1}]$ is a codeword iff $cH^T = 0$. A toy example of the parity check matrix is shown in Fig. 2(a). For real LDPC codes used in practical systems, n is at least a few thousands and the parity check matrix H is large and very sparse. The H matrix can be also represented by a Tanner graph as shown in Fig. 2(b). Each row of H is represented by a check node in the Tanner graph and specifies a check equation that needs to be satisfied. Each column of H corresponds to a variable node. Each nonzero entry in H represents the connection edge between the corresponding check node and variable node. The inputs to the LDPC decoder from the channel are the probabilities that each received bit is ‘1’. During the decoding process, probability messages are passed between the connected variable and check nodes and got

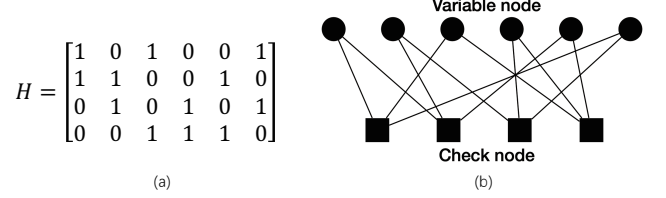


Fig. 2. (a). a toy example of parity check matrix; (b) Tanner graph of the example parity check matrix

Algorithm 1 The Min-sum Decoding Algorithm

```

1: initialization:  $u_{m,n} = \gamma_n$ ;  $z_n = \text{sign}(\gamma_n)$ 
2: for  $i = 1$  to  $I_{\max}$  do
3:   Compute  $zH^T$ ; Stop and return  $z$  if  $zH^T = 0$ 
4:   check node processing
5:    $\min1_m = \min_{j \in S_v(m)} |u_{m,j}|$ 
6:    $idx_m = \text{argmin}_{j \in S_v(m)} |u_{m,j}|$ 
7:    $\min2_m = \min_{j \in S_v(m), j \neq idx_m} |u_{m,j}|$ 
8:    $s_m = \prod_{j \in S_v(m)} \text{sign}(u_{m,j})$ 
9:   for all  $n \in S_v(m)$  do
10:     $|v_{m,n}| = \begin{cases} \alpha \min1_m & \text{if } n \neq idx_m \\ \alpha \min2_m & \text{if } n = idx_m \end{cases}$ 
11:     $\text{sign}(v_{m,n}) = s_m \text{sign}(u_{m,n})$ 
12:   end for
13:   variable node processing
14:    $u_{m,n} = \gamma_n + \sum_{i \in S_c(n), i \neq m} v_{i,n}$ 
15:   a posteriori info. comp. & tentative decision
16:    $\tilde{\gamma}_n = \gamma_n + \sum_{i \in S_c(n)} v_{i,n}$ 
17:    $z_n = \text{sign}(\tilde{\gamma}_n)$ 
18: end for

```

updated iteratively. At the end of each iteration, hard decisions are made based on the most updated messages. If the hard-decision vector, z , satisfies $zH^T = 0$, then z is the correct codeword and the decoding stops. Otherwise, the decoding process repeats until the pre-set maximum iteration number, I_{\max} , in which case decoding failure is declared.

LDPC codes can be decoded by many different decoding algorithms. The most popular one is the Min-sum decoding algorithm [18], since it can well balance the complexity and the error-correcting performance. Denote the message from variable node n to check node m by $u_{m,n}$. Represent the message from check node m to variable node n by $v_{m,n}$. The channel information γ_n is the log-likelihood ratio of the probability that the n -th input bit is ‘1’ over the probability that it equals ‘0’. $S_c(n)(S_v(m))$ represents the set of check (variable) nodes connected to variable (check) nodes $n(m)$. The pseudo codes of the Min-sum algorithm are listed in Algorithm 1.

In the beginning of the decoding process, the variable-to-check (v2c) messages are initialized and hard decisions are first made according to the channel inputs γ_n . Test is carried out to see if the hard-decision vector is a codeword. If not, the iterative process starts. Each decoding iteration is divided into three steps. For each check node m , the check node processing step finds the smallest and the second smallest of $|u_{m,j}|$, which are denoted by $\min1_m$ and $\min2_m$, respectively, among the

messages from all connected variable nodes. Besides, the index of the smallest $|u_{m,j}|$ is derived as idx_m . Then the check-to-variable (c2v) messages are computed according to Lines 9-12 of Algorithm 1. $min1_m$ and $min2_m$ are scaled by pre-determined constant $0 < \alpha < 1$ to improve the error-correcting performance. In the variable node processing step, $u_{m,n}$ is updated by adding the channel information with the newly computed c2v messages from all connected check nodes, except check node m . The *a posteriori* information, $\tilde{\gamma}_n$, is computed in a similar way except that none of the c2v messages is excluded. Then the hard decision, z_n , equals the sign of $\tilde{\gamma}_n$. When the hard-decision vector satisfies $zH^T = 0$, the correct codeword is found and the decoding stops.

III. SECURE OBFUSCATION SCHEMES FOR LDPC DECODERS

A. Ineffectiveness of existing logic locking

In the secure integration mode [7], the inputs of the logic-locking block are normally connected to the primary inputs of the target circuit as shown in Fig. 4(a). The output of the logic-locking block is usually XORed with a signal in the circuit that can effectively affect the overall output. Since the decoding results are hard decisions of the messages, the sign product, s_m , and the most significant bit (MSB) of $min1_m$ are among the signals that affect the Min-sum decoding results most. To find the effects of flipping these signals by logic locking on the performance of the Min-sum decoder, simulations are carried out over the binary symmetric channel for an example (1270, 635) quasi-cyclic (QC)-LDPC code, whose H matrix consists of 5×10 shifted identity matrices of dimension 127×127 . QC-LDPC codes are usually used in practical applications because the structure of their H matrices allows efficient parallel processing. I_{max} is set to 15 as in typical settings. In our simulations, a random check node is picked and its sign product or the MSB of the $min1$ value is flipped in every iteration. The frame error rate (FER) and average number of iterations are the two criteria used to measure the performance of the LDPC decoder. They are plotted in Fig. 3 for the example code over a range of input bit error rates (BERs). For each BER, simulations are run until at least 10 frame errors have been collected to find the FER. This means, for example, more than 10^7 decoding samples have been run for $BER=0.025$.

From Fig. 3, it can be observed that even if the sign product or the MSB of $min1$ of a check node is flipped in every iteration, the resulted differences in the FER and throughput are negligible. The reason is that the LDPC decoder is self-correcting. Even if a c2v message becomes wrong because of the flipping, the other c2v messages sent to the same variable node and the channel information are added up to compute the v2c message and the *a posteriori* information as in Lines 14 and 16 of Algorithm 1. Only the minimum and second minimum magnitudes of the v2c messages affect later decoding iterations. As a result, the chance that the decoding needs more iterations or become unconvergeable is very low. None of the existing logic-locking schemes can make the output wrong for every input pattern when a wrong key is

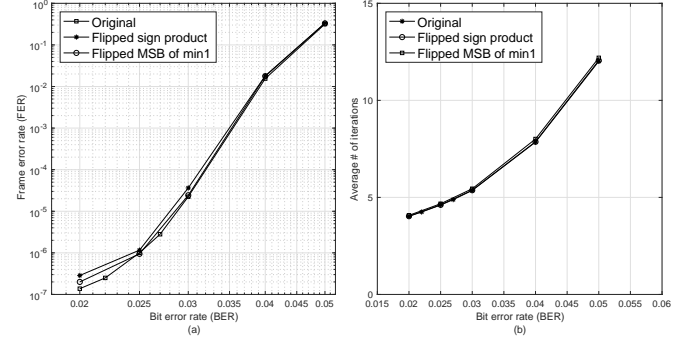


Fig. 3. Simulation results for (1270, 635) QC-LDPC code: (a) FERs; (b) average number of iterations; for original decoder and decoders with sign product and MSB of $min1$ flipped for one check node in every iteration with $I_{max} = 15$

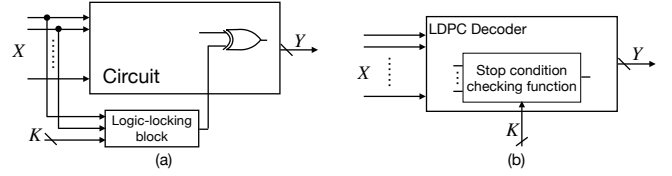


Fig. 4. (a) obfuscated circuit by using existing logic-locking blocks; (b) obfuscated LDPC decoder by locking the stop condition checking function

used. Hence, the resulted FER and throughput degradations would be even less significant compared to those shown in Fig. 3.

Existing logic-locking methods are done in logic level without considering the function implemented by the circuit. In the case that the algorithm is self-correcting or fault-tolerating, any random key can be used for such logic-locking schemes without affecting the system performance much as shown in the above example. To substantially degrade the system performance when the key is incorrect, logic-locking methods incorporating the properties of the algorithm are necessary. Two algorithmic obfuscation schemes for LDPC decoders are introduced in the next two subsections. By locking the stop condition checking function, the designs proposed next can significantly degrade the throughput and/or error-correcting performance when the wrong key is applied. Besides, by modifying the decoding stop condition, our designs effectively resist removal attacks.

B. Obfuscated LDPC decoder with throughput degradation at wrong keys

The Min-sum decoding algorithm is iterative. Let $t = zH^T$. The decoding stops when $t = 0$ and the most updated z vector is the correct codeword. If t does not become zero, the decoding runs until the pre-set maximized number (I_{max}) of iterations, in which case decoding failure is declared. In the proposed design, as shown in Fig. 4(b), the stop condition is controlled by a key vector and it is changed when the wrong key is applied. Applying a wrong key leads to one of the two effects: 1) even though the correct codeword is already found, the decoding still run until the last iteration; 2) the

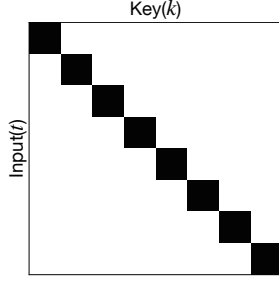


Fig. 5. The K-map pattern of function $f_1(t, k)$

decoding process terminates before the correct codeword is found. The first case does not affect the error-correcting performance but reduces the throughput of the decoder. The second case increases the decoding failure rate. Hence, replacing the original stop condition ($t == 0$) checking function by a key controlled stop condition checking can effectively obfuscate LDPC decoders. Next, our first key-controlled stop condition logic-locking scheme is presented.

The original stop condition is $t == 0$. If t has h bits, the original stop condition checking function is

$$f(t) = \overline{t_0} \& \overline{t_1} \& \cdots \& \overline{t_{h-1}}. \quad (2)$$

By adding a constant vector, v , decided by the designer and slightly modifying the LDPC decoding algorithm as will be detailed in subsection D of this section, the decoding converges when $t == vH^T$. Our first obfuscation method locks the stop condition checking function by $t == k$. It means that the right key is vH^T and only when the vector t equals the key input, k , the LDPC decoding will stop. The Boolean expression of our logic-locking function is

$$f_1(t, k) = \overline{(t_0 \oplus k_0)} \& \overline{(t_1 \oplus k_1)} \& \cdots \& \overline{(t_{h-1} \oplus k_{h-1})} \quad (3)$$

The K-map pattern of the $f_1(t, k)$ function is shown in Fig. 5. The black cells in Fig. 5 mean that $f_1(t, k)$ is ‘1’ for the corresponding key and input, in which case the LDPC decoding stops.

When the stop condition checking function is locked by $f_1(t, k)$, using a wrong key changes the stop condition. For a given wrong key, the decoding will only stop when the syndrome t equals the wrong key. Hence, most likely, the LDPC decoding will run to the last iteration. However, the original LDPC decoding will not run until the last iteration in most cases at the operating region. As shown for the example code in Fig. 3, even though I_{max} is set to 15 to achieve good error-correcting capability, the decoding takes on average around 5 iterations to converge for the practical operating range of $FER < 10^{-4}$. Hence the throughput of the obfuscated LDPC decoder is significantly decreased when a wrong key is used. On the other hand, since the LDPC decoding converges in less than I_{max} iterations when a wrong key is used, except in the case that t accidentally equals the wrong key, or run until the last iteration anyway in undecodable cases, the obfuscated decoder output, z , is not much different from the original decoding result and the FER is almost the same. In our designs, the corruptibility

of a wrong key is defined in terms of the number of input patterns leading to the wrong decoder output regardless of the number of decoding iterations. Hence, the wrong keys in our first proposed design all have low corruptibility.

The size of the key input is equal to the number of rows in the parity check matrix of the LDPC code in the above scheme. For practical LDPC codes, the H matrix has hundreds or even thousands of rows. Using such a long key leads to high logic complexity and requires large memory. To address this issue, a shorter key input can be used to lock parts of the bits in t . Assume that the size of t is h bits, and the size of key input is reduced to $h_k < h$ bits. Then the key-controlled function $f_1(t, k)$ can be modified to

$$f_2(t, k) = \overline{(t_0 \oplus k_0)} \& \cdots \& \overline{(t_{h_k-1} \oplus k_{h_k-1})} \& \overline{t_{h_k}} \& \cdots \& \overline{t_h}, \quad (4)$$

where $\hat{t}_i = t_i$ or \bar{t}_i when the corresponding bit in vH^T is ‘1’ or ‘0’, respectively. The LDPC decoding stops when the first h_k bits of t equal the key input bits and the other bits are the same as those in vH^T . Using an h_k that is large enough can still effectively reduce the throughput substantially and resist various attacks.

C. Obfuscated LDPC decoder with error-correcting performance and throughput degradation at wrong keys

In our first obfuscation method, all wrong keys are of low corruptibility and the resulted error-correcting performance degradation is negligible. Next, a second design with high-corruptibility wrong keys is proposed. The high-corruptibility wrong keys make the decoder prematurely stop at multiple values of the t vector before the codeword is found. As a result, the error-correcting performance of the obfuscated LDPC decoder is significantly degraded when a wrong key is used. Besides, similar to the first design, a wrong key leads to substantial reduction on the decoding throughput since the decoding will run until the last iteration in most cases.

The decoder input hard decision is $z = c \oplus e$, where e is the error vector. For practical channel BERs, the number of errors happened is small. Hence, $t = zH^T = (c \oplus e)H^T = eH^T$ has limited number of patterns and the patterns are not randomly distributed. Take the (1270, 635) LDPC code in Fig. 3 as an example. If the FER needs to be lower than 10^{-6} , then the BER should be around or less than 0.025. For this code with row weight 10, it can be computed that the probability of each bit of t being ‘1’ is $\sum_{i=1,3,5,7,9} \binom{10}{i} \times 0.025^i \times 0.975^{10-i} \approx 0.201$. Hence, t has lower Hamming weight in most of the cases. If t is directly used as the input of the logic-locking block and a random wrong key is picked, then most likely the wrong key will not make the decoding stop prematurely and the error-correcting performance of the decoder will not change much.

To substantially degrade the LDPC decoder error-correcting performance, the vector t needs to be mapped to a randomly-distributed vector, r , to be used as the input of the logic-locking block. In other words, the mapping should be designed such that $Pr\{r_i = 1\} \approx 0.5$. Divide the t vector into groups of g bits. In our design, $r_i = t_{i \times g} \oplus t_{i \times g + 1} \oplus \cdots \oplus$

$t_{i \times g+g-1}$, and g is chosen to make $\Pr\{r_i = 1\} \approx 0.5$. Take the (1270, 635) LDPC code in Fig. 3 as an example, when $BER = 0.025$, $\Pr\{r_i = 1\}$ can be calculated as $\sum_{j=0}^{2j+1 < g} \binom{g}{2j+1} 0.201^{2j+1} (1 - 0.201)^{g-2j-1}$. $\Pr\{r_i = 1\} \approx 0.499$, which is around 0.5, by using $g = 15$. For a different BER and/or an LDPC code with different row weight, g can be selected in a similar way. Changing the stop condition to a nonzero vector as will be detailed in the next subsection does not affect this mapping function or the value of g .

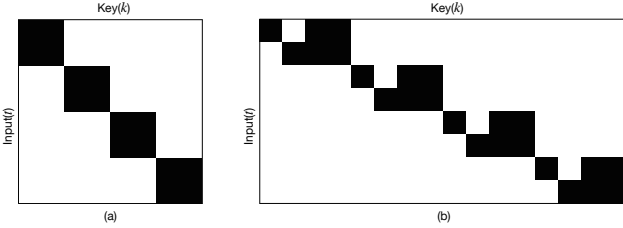


Fig. 6. (a) The K-map of the f_3 function with only high-corruptibility wrong keys; (b) the K-map of the f_4 function

Assume that l_r bits of r are generated from t through the mapping. If the logic-locking block is to make the decoding stop when the key equals the input as in our first proposed scheme, then its function making use of r is

$$f_3(r, k) = \overline{(r_0 \oplus k_0) \& \dots \& (r_{l_r-1} \oplus k_{l_r-1})}.$$

Each key makes the decoding stop at one pattern of r . If the number of rows in the parity check matrix of the LDPC code is h , each pattern of r corresponds to 2^{h-l_r} patterns of t . Therefore, as shown in the K-map of the f_3 function in Fig. 6(a), each wrong key has high corruptibility and makes the decoding stop at 2^{h-l_r} different patterns of t . The probability that the LDPC decoding process stops in each iteration is upper bounded by $1/2^{l_r}$ and it most likely decreases over the iterations since the Hamming weight of t is becoming lower. Since the FERs required for practical applications are low, such as less than 10^{-5} or 10^{-6} , the wrong keys lead to significant increase in the FERs. Smaller l_r degrades the FER more. On the other hand, the wrong keys with higher corruptibility are more likely to be excluded within a small number of iterations in the AppSAT attack [9]. A proper value needs to be picked for l_r to balance the FER degradation and AppSAT attack resistance. Besides, the decoding always runs until the last iteration when r does not equal the wrong key. Hence, the high corruptibility wrong keys also reduce the throughput of the LDPC decoder.

If all wrong keys have high corruptibility as shown in Fig. 6(a), the SAT resistance cannot be guaranteed. Wrong keys with corruptibility as one need to be introduced to resist the SAT attack [11]. Each wrong key for function f_2 (4) makes the LDPC decoding stop at one pattern of t . Such a function can be utilized to introduce wrong keys of corruptibility one. The logic-locking function of our second obfuscation scheme is

$$f_4(t, k) = f_3(r, kb) \& (f_2(t, ka) + f_h(r, ka)), \quad (5)$$

where $k = [kb||ka]$. Similarly, kb has l_r bits. Since the l_r bits of r are generated from gl_r bits of t , the key length of

ka is set to gl_r . ka can be also made longer at the cost of higher logic complexity and larger memory for storing the key. In (5), $f_h(r, ka) = (r_0 \oplus ka_0 \oplus \dots \oplus ka_{g-1}) + \dots + (r_{l_r-1} \oplus ka_{g(l_r-1)} \oplus \dots \oplus ka_{gl_r-1})$ is ANDed with f_3 to make the high-corruptibility wrong keys of f_4 have the same corruptibility as the wrong keys of the f_3 function. The K-map of f_4 is shown in Fig. 6(b). By ANDing $f_3(r, kb)$ with $f_2(t, ka)$, $f_4 = 1$ in the cells of the K-map whose labels satisfy that $kb = r, ka = [t_0 \dots t_{gl_r-1}]$, and the other bits of t equal the corresponding bits of vH^T . These cells are the single black cells in the respective columns in Fig. 6(b) and their column labels are the low-corruptibility keys. $f_3(r, kb) \& f_h(r, ka)$ makes $f_4 = 1$ in the cells whose labels satisfy that $kb = r, [(ka_0 \oplus \dots \oplus ka_{g-1}), \dots, (ka_{g(l_r-1)} \oplus \dots \oplus ka_{gl_r-1})] \neq r$. The column labels for these cells are the high-corruptibility keys.

Using the f_4 function, the keys are divided into three categories: 1) a single correct key that makes the LDPC decoding stops at $t == vH^T$; 2) the low-corruptibility wrong keys that affect the error-correcting performance of the LDPC decoder negligibly but reduce the throughput; 3) the high-corruptibility wrong keys that not only degrade the error-correcting performance but also reduce the throughput. The ratio between the high-corruptibility and the low-corruptibility wrong keys is affected by l_r . When l_r is larger, the ratio is larger. However, the corruptibility of the high-corruptibility wrong keys is reduced and hence the degradation on the error-correcting performance is less significant. l_r allows a tradeoff between the corruptibility of the wrong keys and portion of high-corruptibility wrong keys. Nevertheless, even if a low-corruptibility wrong key is used, there is significant degradation on the throughput and the decoder cannot achieve the target speed.

D. Min-sum algorithm with modified stop condition

The main idea of the two proposed obfuscation methods is to lock the stop condition checking function by a key and the correct key equals the syndrome when the decoding converge. The stop condition for the original LDPC decoder is $t == 0$. A potential threat is that the zero stop condition can be easily guessed by an attacker who has knowledge about LDPC decoders. If the stop condition checking logic-locking block can be identified from the netlist, then it can be eliminated and replaced by a zero detector. Next, low-overhead modifications to the LDPC decoding algorithm are proposed to address this issue.

In our design, a constant vector, v , chosen by the designer is added to the input vector $z = c \oplus e$. Hence the decoding is carried out on $z' = c \oplus e \oplus v$. The decoding algorithm can be modified so that it generates $c \oplus v$ when the error vector, e , is decodable. Then c can be recovered by adding v back. Such modifications lead to exactly the same decoding results and do not cause any error-correcting performance loss. However, in this case, the correct stop condition is changed to whether t equals $p = vH^T$, which is not an all-'0' vector. To incorporate the v vector, the Min-sum decoding can be modified as in Algorithm 2. At initialization, v is added to $sign(\gamma_n)$ to

Algorithm 2 The Modified Min-sum Decoding Algorithm

```

1: initialization:  $|\gamma'_n| = |\gamma_n|$ ;  $\mathbf{z}'_n = \text{sign}(\gamma'_n) = \text{sign}(\gamma_n) \oplus \mathbf{v}_n$ 
    $u'_{m,n} = \gamma'_n$ 
2: for  $k = 1$  to  $I_{max}$  do
3:   Compute  $\mathbf{z}'H^T$ ; Stop & return  $\mathbf{z}' \oplus \mathbf{v}$  if  $\mathbf{z}'H^T = \mathbf{p}$ 
4:   check node processing
5:    $min1'_m = \min_{j \in S_v(m)} |u'_{m,j}|$ 
6:    $idx'_m = \operatorname{argmin}_{j \in S_v(m)} |u'_{m,j}|$ 
7:    $min2'_m = \min_{j \in S_v(m), j \neq idx'_m} |u'_{m,j}|$ 
8:    $s'_m = (-1)^{p_m} \prod_{j \in S_v(m)} \text{sign}(u'_{m,j})$ 
9:   for all  $n \in S_v(m)$  do
10:     $|v'_{m,n}| = \begin{cases} \alpha min1'_m & \text{if } n \neq idx'_m \\ \alpha min2'_m & \text{if } n = idx'_m \end{cases}$ 
11:     $\text{sign}(v'_{m,n}) = s'_m \text{sign}(u'_{m,n})$ 
12:  end for
13:  variable node processing
14:   $u'_{m,n} = \gamma'_n + \sum_{i \in S_c(n), i \neq m} v'_{i,n}$ 
15:  a posteriori info. comp. & tentative decision
16:   $\tilde{\gamma}'_n = \gamma'_n + \sum_{i \in S_c(n)} v'_{i,n}$ 
17:   $z'_n = \text{sign}(\tilde{\gamma}'_n)$ 
18: end for

```

generate the initial hard-decision vector z' and $|\gamma'_n| = |\gamma_n|$. Accordingly, the initial $u'_{m,n}$ equals γ'_n . In the first iteration, $min1'_m$, idx'_m and $min2'_m$ are computed in the same way and they equal to the $min1_m$, idx_m and $min2_m$, respectively, in Algorithm 1, since the magnitudes of the channel information do not change. By multiplying $(-1)^{p_m}$ to the product of signs, the s'_m computed from Line 8 of Algorithm 2 also equals the s_m in Algorithm 1. The signs of all the messages added up in the variable node processing and *a posteriori* information computation from Algorithm 2 are different from those in Algorithm 1 by v_n . As a result, the z' vector in Algorithm 2 and the z vector in Algorithm 1 is always different by v in every iteration. Hence, by adding v back after the decoding, the same codeword is generated.

QC-LDPC codes [19] are usually used in practical systems since they enable efficient parallel processing. The H matrix of a QC-LDPC code consists of sub-matrices, each of which is either a zero or a cyclically shifted identity of dimension $q \times q$. Most parallel LDPC decoder designs process one submatrix or one block column of sub-matrices in each clock cycle. To reduce the storage requirement, v can be a vector with repeated patterns of length q . In this case, the addition of v to the input and output, as well as the modifications on the sign products in the Min-sum decoding algorithm can be implemented by adding NOT gates according to the pattern of v to the decoder circuits and no memory is required to store v . Besides, inverters are combined with the other logic gates by the synthesis tool and they are not visible from the netlist. Hence, the vector v can not be easily recovered from the netlist. Additionally, adding NOT gates does not necessarily increase the area since inverting gates, such as NAND and NOR, are smaller than non-inverting gates, such as AND and OR.

IV. SECURITY AND COMPLEXITY ANALYSE

This section analyzes the security and complexity of the proposed obfuscated LDPC decoders by using an example (1270, 635) QC-LDPC code. The H matrix of this code consists of 5×10 sub-matrices of dimension 127×127 .

A. SAT and AppSAT attack resistance

Due to the large size of the LDPC decoder and that the iterative process needs to be unrolled, which increases the circuit size proportionally with I_{max} , it is infeasible to carry out SAT and AppSAT attack experiments on the proposed designs. In this section, mathematical analyses are carried out on the resiliency of the proposed designs to the SAT and AppSAT attacks.

The main idea of the SAT attack is to exclude all wrong keys that make the obfuscated output different from the original output. For LDPC decoders, whether an output equals the original output is determined based on the returned codeword vector without taking into account the number of decoding iterations. The keys incapable of making the output different from the original output cannot be excluded by the SAT attack. In the proposed obfuscated LDPC decoders, $t = z'H^T = (e \oplus v)H^T$. Under practical operating channel condition, e has a small number of nonzero bits. In this case, t only has a limited number of possible patterns. Accordingly, most of the low-corruptibility wrong keys lead to the same decoding output vector although the decoding runs until the last iteration. These wrong keys can not be excluded by the SAT attack. As a result, after the SAT attack stops, there is a large number of low-corruptibility wrong keys left in the pool. Using any of them makes the decoder run to the last iteration and causes significant degradation on the decoding throughput. For the (1270, 635) example code, when $BER = 0.02$, the error vector e has 25 '1's on average. There are around $\binom{1270}{25} \approx 2^{170}$ patterns of e with 25 '1's and the corresponding 635-bit t vector has at most 2^{170} different patterns. If the h_k in our first proposed design is set to 127, then there are 2^{127} possible keys. The key bits are compared to the first 127 bits of t , which has $2^{170} \times 127/635 = 2^{34}$ possible patterns assuming that the '1's in the t vector are evenly distributed. Therefore, at most 2^{34} wrong keys can be excluded by the SAT attack. Each of the remaining $2^{127} - 2^{34} - 1$ wrong keys would make the decoding run until the last iteration. If the attacker can abuse the decoder and use any vector as e without restriction on the number of '1's, then the number of possible patterns of t substantially increases. In this case, more wrong keys will be excluded by the SAT attack. However, the number of iterations in the SAT attack is exponential to the number of key bits. The second proposed design also has 2^{gl_r} wrong keys of corruptibility one and has similar resistance to the SAT attack.

All wrong keys for the first proposed obfuscated decoder have low corruptibility. If the AppSAT attack is applied, any returned key has low corruptibility. A low-corruptibility key most likely makes the decoder run until the last iteration and leads to significant decrease in the throughput. The ratio between the high-corruptibility and low-corruptibility wrong keys in the second proposed design is around 2^{lr} . Although

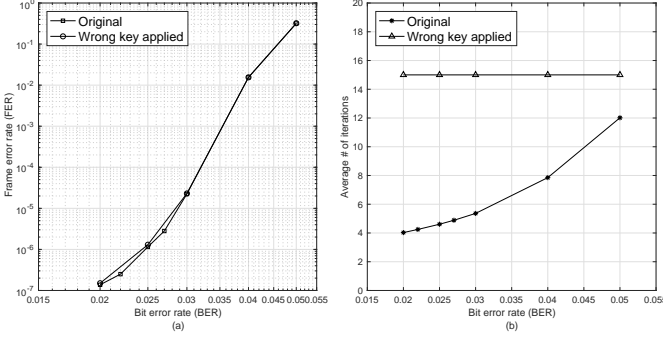


Fig. 7. Min-sum decoding results for (1270, 635) QC-LDPC code with $I_{max} = 15$ using the first proposed obfuscation scheme that only has low-corruptibility wrong keys: (a) frame error rate; (b) average number of iterations

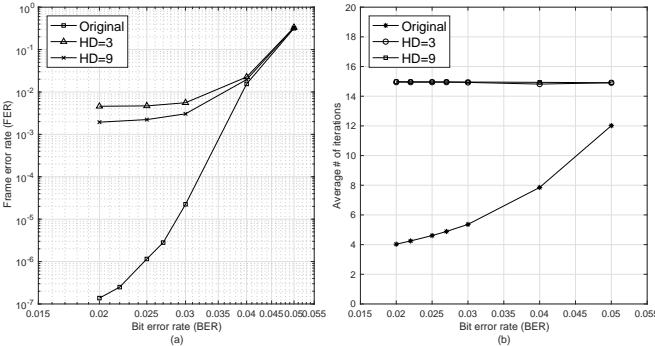


Fig. 8. Min-sum decoding results for (1270, 635) QC-LDPC code with $I_{max} = 15$ using the second proposed obfuscation scheme that has both high and low-corruptibility wrong keys: (a) frame error rate; (b) average number of iterations

high-corruptibility wrong keys are more likely to be excluded by the AppSAT attack, some high-corruptibility wrong keys are left in the pool. If a high-corruptibility wrong key is returned by the AppSAT attack and is used for the decoder, it will lead to degradation on not only the throughput but also the FER of the decoder. If a low-corruptibility wrong key is returned, then the throughput is degraded. For either case, the returned key is not usable.

Simulation results for the first obfuscated LDPC decoder whose wrong keys are all of low corruptibility are shown in Fig. 7. The example (1270, 635) code is used and I_{max} is set to 15 iterations in our simulations. As illustrated in Fig. 7 (b), in the original LDPC decoder, the average number of decoding iterations is much smaller than I_{max} . However, if a wrong key is used, the decoder most likely runs until the last iteration and the average number of iterations becomes almost I_{max} . For the practical operating range of $BER < 0.03$, this translates to more than three times reduction on the throughput. On the other hand, each wrong key makes the decoder stop at one pattern of t , and the chance that the decoding stops prematurely at a wrong vector is small. As a result, as shown in Fig. 7(a), the first proposed obfuscation only leads to negligible difference in the FER.

In the second proposed design, if a low-corruptibility wrong key is picked, the decoder will have significant degradation on

the throughput but negligible difference in the FER similar to those in Fig. 7. To show the effects of the high-corruptibility wrong keys in the second design on the FERs, simulation results with l_r set to 10 are illustrated in Fig. 8. Two wrong keys with Hamming distance (HD) 3 and 9 in the kb part from the vector r computed using $t = vH^T$ are selected randomly in these simulations. The corruptibilities of these two wrong keys are both $2^{h-l_r} = 2^{625}$. However, the one with smaller HD causes more degradation on the FER as shown in Fig. 8(a). The reason is that the number of errors decreases and the HD between t and vH^T becomes lower over the LDPC decoding iterations. When a wrong key with smaller HD is used, the chance that it equals the r vector and makes the decoding stop prematurely is higher compared to the case that a key with higher HD is utilized. Nevertheless, even for the almost largest possible HD=9 that can be used when $l_r = 10$, the wrong key leads to more than two orders of magnitude degradation on the FER at practical operating range of $BER < 0.03$. The probability that a high-corruptibility wrong key makes the decoding stop prematurely is also relatively small and hence the decoding also runs until the last iterations in most cases. Therefore, as shown in Fig. 8(b), the average number of iterations is also around 15 when high-corruptibility wrong keys are used. The average iteration number for the HD=3 wrong key is slightly lower compared to the case of HD=9, although the difference is not visible from the figure.

B. Removal attack resistance

Both of the proposed schemes obfuscate LDPC decoders in algorithmic level instead of just adding a logic-locking block to the circuit. It is possible that the block or part of the block implementing the function f_2 or f_4 can be identified, for example, by sorting the SPS values of the signals, since it involves large AND trees. However, these functions check the stop condition and they are integral parts of the decoder. If they are removed, the LDPC decoder will run until the last iteration and the throughput is substantially reduced. Additionally, by modifying the decoding algorithm with negligible complexity overhead, the stop condition is changed from an all-'0' vector to a random-like vector. This makes it impossible to replace the proposed logic-locking block by the correct function even if the attacker knows that a normal LDPC decoder stops at all-'0' syndrome vector. Besides, the NOT gates inserted for the algorithmic modifications are combined with the other logic gates by the synthesis tool. Hence, the v vector and accordingly the modified stop condition can not be recovered from the netlist either.

C. Complexity analysis

This section analyzes the overheads of the proposed obfuscation schemes brought to the example LDPC decoder.

The hardware implementation architectures of LDPC decoders depend on not only the decoding algorithm but also the computation scheduling scheme. Sliced message-passing is a popular LDPC decoding scheduling scheme due to its high throughput and low memory requirement [20]. In such a decoder, one block column of the H matrix is processed

in each clock cycle. Hence, $5 \times 127 = 635$ check node units (CNUs) are used to compute the $min1_m$, $min2_m$, etc. and then derive the c2v messages for each row of the H matrix in parallel. Also 127 variable node units (VNUs) are used to compute the v2c messages and the *a posteriori information*. Besides, 2×5 127-input Barrel shifters are needed to route the messages between the CNUs and VNUs according to the offsets of the shifted identity sub-matrices in H . Details about the CNU and VNU can be found in [20]. Assume that each NAND or NOR gate is implemented by half of the area of an XOR, each 1-bit 2-to-1 multiplexer takes the same area of an XOR, and each register with pre-set and clear pins requires three time the area of the XOR. The complexity of the logic gates and registers required by the original slide-message-passing LDPC decoder can be estimated as shown in Table I.

TABLE I
AREA COMPLEXITY OF SLICED-MESSAGE-PASSING LDPC DECODERS FOR
(1270,635) CODE

	XOR Gate Count
CNUs	60642
VNUs	42545
routing networks	35840
stop condition checking block	317
Original decoder total gate count	139344
Overhead of first obfuscated decoder	127 (0.09%)
Overhead of second obfuscated decoder	460 (0.33%)

The first proposed obfuscation scheme uses the $f_2(t, k)$ function (4) to implement the stop condition checking. Compared to the original stop condition checking function $f(t)$ in (2), the overheads include h_k XOR gates. h_k is the number of key bits in the first proposed scheme and it affects the achievable security level. Even when h_k is set to 127, the proposed obfuscation scheme only brings $127/139344 = 0.09\%$ overhead to the logic complexity. Besides the computation units listed in Table I, large memories are needed to store the channel input of the decoder and the hard-decision vector. Hence, the overhead brought by the proposed scheme to the overall decoder area is even smaller. As mentioned previously, the modifications on the LDPC decoding algorithm for changing the stop condition are implemented by adding NOT gates, which are often combined into other gates by the synthesis tool. Hence those NOT gates do not necessarily cause any area overhead.

The $f_2(t, k)$ function has one more gate in the data path compared to $f(t)$. However, the VNUs have several multi-bit adders and two sign-magnitude to 2's complement converters in the data path. It is much longer than the data path of the stop condition checking and decides the critical path of the LDPC decoder. Therefore, the proposed scheme does not cause any degradation on the achievable clock frequency of the decoder.

The second proposed obfuscation scheme is done by utilizing the $f_4(t, k)$ function (5). When the values of g and l_r are set to 15 and 10, respectively, the sizes of ka and kb are 10 and 150 bits, respectively. Each bit of r is the XOR result of g bits of t , and hence mapping t to r needs $l_r \times (g-1) = 140$ XOR gates. Beside, the f_2 and f_3 parts in

the $f_4(t, k)$ formula require an additional $ka+kb = 160$ XOR and $l_r-1 = 9$ AND gates compared to the $f(t)$ function. Also the f_h part requires $g \times l_r = 150$ XOR and $l_r-1 = 9$ OR gates to implement. Overall, the $f_4(t, k)$ function needs around 460 extra XOR gates to implement compared to the original stop condition checking function $f(t)$. This overhead is only $460/139344 = 0.33\%$ of the overall LDPC logic complexity.

V. DISCUSSIONS

Using an existing logic-locking scheme, such as the Anti-SAT, G-Anti-SAT, DTL, or SFLL design, to lock one bit of t does not effectively corrupt the LDPC decoder output. Flipping one bit of t makes the LDPC decoding stop at a wrong pattern of t . However, the chance that t equals a pattern with a single nonzero bit is very low. Hence, such logic-locking method does not lead to any noticeable increase in the FER. Besides, the outputs of existing lock-locking blocks are not always '1'. Even if a scheme with relatively high corruptibility, such as the DTL design [9], is used, the selected bit of t will not be flipped with high probability. Hence, even if the decoder stops at a later iteration, only one or two more iterations are carried out instead of until the last iteration. Accordingly, existing logic-locking schemes do not cause significant throughput degradation as the proposed designs.

Another possible method to obfuscate the LDPC decoder is to XOR the output of an existing logic-locking block directly with one bit in the decoder output vector. However, by comparing the output of the locked decoder with that of a functioning decoder, the location of the flipped bit can be easily identified and the logic-locking block can be easily removed.

VI. CONCLUSIONS

In this paper, two algorithmic obfuscation schemes for LDPC decoders have been proposed by locking the stop condition checking function and modifying the decoding algorithm. Both designs have low-corruptibility wrong keys that cannot be all excluded by the SAT or AppSAT attacks. Those wrong keys lead to significant degradation on the decoder throughput. In addition to the low-corruptibility wrong keys, there are a large portion of high-corruptibility wrong keys in the second proposed obfuscation method. They cause significant degradations on not only the throughput but also the error-correcting performance. Besides, the proposed modifications on the decoding algorithm make the correct decoding stop condition a secret and thwart possible attacks. Future work will study algorithmic obfuscations on other fault-tolerating or self-correcting functions.

REFERENCES

- [1] J. A. Roy, F. Koushanfar, and I. L. Markov, "EPIC: ending piracy of integrated circuits," *Proc. Conf. on Design, Automation and Test in Europe*, pp. 1069-1074, Munich, Germany, 2008.
- [2] P. Subramanyan, S. Ray, and S. Malik, "Evaluating the security of logic encryption algorithms," *Proc. IEEE Intl. Symp. on Hardware Oriented Security and Trust*, pp. 137-143, Washington DC, U.S.A., 2015.
- [3] J. Rajendran, Y. Pino, O. Sinanoglu and R. Karri "Security analysis of logic obfuscation," *Proc. of ACM/EDAC/IEEE Design Automation Conf.*, pp. 83-89, San Francisco, CA, U.S.A., 2012.

[4] J. Rajendran *et. al.*, "Fault analysis-based logic encryption," *IEEE Trans. on Computers*, vol. 64, no. 2, pp. 410-424, Feb. 2015.

[5] Y. Lee and N. A. Touba, "Improving logic obfuscation via logic cone analysis," *Proc. Latin-American Test Symposium*, pp. 1-6, Puerto Vallarta, Mexico, 2015.

[6] B. Liu and B. Wang, "Embedded reconfigurable logic for ASIC design obfuscation against supply chain attacks," *Proc. Conf. on Design, Automation and Test in Europe*, pp. 1-6, Dresden, Germany, 2014.

[7] Y. Xie and A. Srivastava, "Anti-SAT: mitigating SAT attack on logic locking," *IEEE Trans. on Computer-Aided Design of Integrated Circuits and Syst.*, vol. 38, no. 2, pp. 199-207, Feb. 2019.

[8] M. Yasin, *et. al.*, "SARlock: SAT attack resistant logic locking," *Proc. IEEE Intl. Symp. on Hardware Oriented Security and Trust*, pp. 236-241, McLean, VA, U.S.A., 2016.

[9] K. Shamsi, *et. al.*, "On the approximation resiliency of logic locking and IC camouflaging schemes," *IEEE Trans. on Information Forensics and Security*, vol. 14, no. 2, pp. 347-359, Feb. 2019.

[10] M. Yasin, *et. al.*, "Removal attacks on logic locking and camouflaging techniques," *IEEE Trans. on Emerging Topics in Computing*, vol. 8, no. 2, pp. 517-532, 1 April-June 2020.

[11] J. Zhou and X. Zhang, "Generalized SAT-attack-resistant logic locking," *Submitted to IEEE Trans. on Information Forensics and Security*.

[12] B. Shakya, *et. al.*, "CAS-Lock: a security-corruptibility trade-off resilient logic locking scheme," *IACR Transactions on Cryptographic Hardware and Embedded Systems*, vol. 2020, issue 1, pp. 175-202.

[13] M. Yasin, *et. al.*, "Provably-secure logic locking: from theory to practice," *Proc. of the ACM SIGSAC Conf. on Computer and Communication Security*, pp. 1601-1618, Dallas, Texas, U.S.A., 2017.

[14] D. Sironi, P. Subramanyan "Functional analysis attacks on logic locking," *IEEE Trans. on Information Forensics and Security*, vol. 15, pp. 2514-2527, Jan. 2020.

[15] R. G. Gallager, "Low density parity check codes," *IRE Trans. Info. Theory*, vol. 8, pp.21-28, Jan., 1962.

[16] Y. Liu, *et. al.*, "Secure and effective logic locking for machine learning applications," *IACR Cryptology ePrint Archive*, 2019

[17] J. Zhou and X. Zhang, "A new logic-locking scheme resilient to gate removal attack," *Proc. IEEE International Symp. on Circuits and Systems*, 2020

[18] J. Chen, M.P.C. Fossorier, "Density evolution for two improved bp-based decoding algorithms of ldpc codes," *IEEE Comm. Letters*, vol. 6, no. 5, pp. 208-210, May 2002

[19] Y. Kou, S. Lin, and M.P.C. Fossorier, "Low-density parity-check codes based on finite geometries: a rediscovery and new results," *IEEE Trans. on Info. Theory*, vol. 47, no. 7, pp. 2711-2736, Jul. 2001

[20] X. Zhang, *VLSI architectures for modern error-correcting codes*, CRC, 2015

PLACE
PHOTO
HERE

Xinmiao Zhang received her Ph.D. degree in Electrical Engineering from the University of Minnesota. She joined The Ohio State University as an Associate Professor in 2017. Prior to that, she was a Timothy E. and Allison L. Schroeder Assistant Professor 2005-2010 and Associate Professor 2010-2013 at Case Western Reserve University. Between her academic positions, she was a Senior Technologist at Western Digital/SanDisk Corporation. Dr. Zhang's research spans the areas of VLSI architecture design, digital storage and communications, security, and signal processing.

Dr. Zhang received an NSF CAREER Award in January 2009. She is also the recipient of the Best Paper Award at 2004 ACM Great Lakes Symposium on VLSI and 2016 International SanDisk Technology Conference. She authored the book "VLSI Architectures for Modern Error-Correcting Codes" (CRC Press, 2015), and co-edited "Wireless Security and Cryptography: Specifications and Implementations" (CRC Press, 2007). She was elected to serve on the Board of Governors of the IEEE Circuits and Systems Society for the 2019-2021 term. She is a Co-Chair of the Data Storage Technical Committee (2017-2020), and a member of the CASCOM and VSA technical committees and DISPS technical committee advisory board of IEEE. She served on the technical program and organization committees of many conferences, including ISCAS, SiPS, ICC, GLOBECOM, GlobalSIP, and GLSVLSI. She has been an associate editor for the IEEE Transactions on Circuits and Systems-I 2010-2019 and IEEE Open Journal of Circuits and Systems since 2019.

PLACE
PHOTO
HERE

Jingbo Zhou received the B.S. degree in telecommunication engineering from Beijing University of Post and Telecommunication, Beijing, China. He is currently pursuing the Ph.D. degree in the Electrical and Computer Engineering Department, The Ohio State University, OH, USA.

His current research interest is hardware security and cryptography.